https://doi.org/10.1016/j.engstruct.2021.112720

Analytical model for circular high strength concrete filled steel tubes under compression

Jiong-Yi ZHU[a], Junbo CHEN[b,c,*] and Tak-Ming CHAN[d]

[a] *Department of Civil Engineering, School of Mechanics and Engineering Science, Shanghai University, Shanghai, China*
[b] *School of Civil and Hydraulic Engineering, Huazhong University of Science and Technology, Wuhan, Hubei, China*
[c] *Formerly, Department of Civil and Environmental Engineering, The Hong Kong Polytechnic University, Hung Hom, Hong Kong*
[d] *Department of Civil and Environmental Engineering, The Hong Kong Polytechnic University, Hung Hom, Hong Kong*

*Corresponding author: junbochen@hust.edu.cn

Abstract

It is well known that the effect of confinement in concrete filled steel tube (CFST) can enhance the axial compressive strength of the concrete core. The confining pressure is a key issue to determine the compressive strength of concrete while the development of confining pressure is related to the lateral responses of steel tube and concrete core. This paper firstly presents a review on the lateral behaviour of circular CFST and existing lateral-axial strain models for concrete. These models are assessed by the authors' previous experimental observations. Assessment results reveal deficiencies of current lateral-axial strain models, especially on the CFST with high strength concrete. A modified lateral-axial strain model for both normal and high strength concrete core in CFST was then proposed to accurately capture the interaction behaviour of the steel tube and the concrete. An analytical model of CFST with uniformly confined concrete core (i.e. with circular section) was then proposed to capture the development of confining pressure in CFST. A reduction factor was considered when the high strength concrete was used. The proposed analytical model can well predict the load bearing capacity, load-shortening curve, axial strain-lateral strain relationship of CFST with normal and high strength concrete.

Keywords: CFST; High strength concrete; Confinement; Analytical model.

1. Introduction

Concrete filled steel tube (CFST) is superior to traditional reinforced concrete columns due to better structural performances from the interaction between concrete and steel. One of the important benefits from the composite action is that the steel tube in CFST can confine the concrete core under compression to enhance the strength and ductility of the concrete. Extensive literature reviews have been conducted on CFST [1-7] and conclude that the effect of confinement is beneficial to the load capacity of CFSTs with circular cross-section shape. The effect of confinement is normally contributed from the lateral confining pressures by the external reinforcements. The popular confining components in existing literature are steel stirrup [8, 9], steel tube [1-3, 6, 10, 11] and fibre-reinforced polymer (FRP) sheet [12, 13]. Researchers [6, 13] investigated the stress-strain relationship of the confined concrete with different external confining components. According to the stress-strain response, the confinement stress-strain model can be categorized into active-confinement model and passive-confinement model. The active-confinement model indicates that the concrete is actively confined with a constant confining pressure and the confining pressure is independent with the lateral stress-strain relationship. The confinement provided by components such as steel stirrups could be classified as passive confinement before yielding and active confinement after yielding because the hoop stress in steel stirrup is constant after yielding. The passive-confinement model indicates that the confining pressure is related to the expansion of concrete core, for instance, in FRP confined concrete the confining pressure is related to the hoop stress in FRP which increases with the increasing of the hoop strain in concrete. In concrete filled steel tube, the confinement is indicated as passive confinement [10, 14], different from steel stirrup, steel tube in CFST is under a biaxial stress state which follows the von Mises yield criterion. After the yielding of the steel tube, the hoop stress is kept increasing with the hoop strain of the concrete core and the axial stress in the steel tube decreases [5, 14]. A well-known concrete stress-strain model was proposed by Mander et al. [8] for the steel stirrup confined (active confined) concrete based on the model proposed by Popovics [15]. This model is applicable to both active confined concrete and unconfined concrete and was served as a base model in the subsequent research to both normal and high strength concrete.

To fully understand the effect of confinement on the enhanced ultimate strength of concrete, a review on the existing literature about ultimate strength of confined concrete has been conducted [8, 9, 13, 16-31]. It should be noted that the base model from Mander et al. [8] is only for the active confined concrete. As for the passive-confinement stress-strain model, a series of stress-strain curves under various confining pressure were firstly developed using the active-confinement model [13, 32], and the corresponding axial stress could then be obtained from these stress-strain curves based on the value of the hoop strain which is related to the confining pressure in passive confinement. To achieve this approach, the hoop strain to axial strain relationship is crucial to the development of passive-confinement model. Teng et al. [13] developed a relationship of the hoop strain and the axial strain of the confined concrete, validated against experimental results with concrete cylinder strength ranging from 32.8-103.3 MPa. This model could be easily adopted in FRP confined concrete as the elastic relationship between the confining pressure and the hoop strain is straightforward due to the unidirectional

property of FRP components. However, in CFST, due to the biaxial stress condition in the steel tube, the confining pressure is not only related to the hoop strain but also related to the axial strain of the column. Recently Kwan et al. [14] proposed a theoretical model through a "trial and error" process to capture the confining pressure in CFST columns. The basic concept of this model is deformation compatibility between the concrete core and the steel tube when the steel tube is confining the concrete core. The equilibrium could be established based on the constitutive models of the concrete core and the steel tube. Based on this model, Kwan et al. [14] indicated that the behaviour of the passively confined concrete core in CFST could be captured.

In recent years, high strength concrete has been increasingly adopted in modern construction. When compared with normal strength concrete, high strength concrete could reduce the column size and free up more lettable floor area especially in high-rise buildings. However, it is indicated that the effect of confinement on the load bearing capacity of CFST is limited by the low steel contribution ratio when high strength concrete is used [33]. Besides the stress-strain behaviour of high strength concrete is also different from that in normal strength concrete. Clark [34] indicated that the divergence of the stress-strain relationship as well as the lateral dilation behaviour from its initial linearity happens at 70% of peak stress for normal strength concrete while the percentage increases to 90 % in high strength concrete. Numerous studies observed that the stress-strain model of confined normal strength concrete is not applicable for the high strength concrete [14, 18, 22, 23, 28, 30].

In summary, based on the current investigations, an incremental numerical procedure to reflect the stress-strain behaviour of confined concrete with both normal and high strength in CFST columns has been developed and is validated by the experimental results.

2. Interaction of concrete core and steel tube in CFST

The interaction of the steel tube and the concrete core in CFST columns is essential to the understanding of the compressive behaviour of the composite column. In current investigations, it is assumed that the axial compression would apply to steel tube and concrete core simultaneously which leads to a same axial shortening of each component during the loading process. Based on this assumption two stages could be recognized in CFST columns under axial compression: unconfined stage and confining stage. At the initial stage of loading, the concentric axial compression is applied to both the steel tube and the in-filled concrete core. As the steel tube expands more than the concrete core in hoop and radial directions due to a higher Poisson's ratio, there is no confining pressure from steel tube to concrete core. Therefore, it can be regarded as unconfined stage. With the increase of axial compression, the axial stress of concrete approaches its ultimate strength and the expansion of the concrete core becomes larger than the steel tube. Eventually, the steel tube starts to confine the concrete core and the lateral stresses are generated in the steel tube. Therefore, the stress condition when the confinement starts is crucial to differentiate the unconfined and confining stages which could be investigated based on accurate lateral-to-axial strain models of steel and concrete.

3. Unconfined stage

It has been observed that the confinement initiates when the lateral strain of concrete reaches the lateral strain of steel tube. To capture the initiation of confinement, the axial strain-to-lateral strain relationship should be developed for each of the components.

3.1 Axial and lateral behaviour of steel

In unconfined stage, the steel tube is under uniaxial compression, where the elastic-perfect plastic model could be adopted for the stress-strain model. The lateral strain of steel tube could be calculated from the Poisson's ratio with the corresponding axial strain because of the uniaxial stress state. For external steel tube, the Poisson's ratio is assumed to be 0.3 in the elastic stage, while the Poisson's ratio at the plastic stage is 0.5 [35]. Thus, the lateral strain at a given axial strain could be obtained from Eqs. 1 and 2:

$$\varepsilon_{l,s} = 0.3\varepsilon_{a,s} \qquad \text{(Elastic stage)} \tag{1}$$

$$\varepsilon_{l,s} = 0.3\varepsilon_{a,se} + 0.5\varepsilon_{a,sp} \qquad \text{(Plastic stage)} \tag{2}$$

where $\varepsilon_{l,s}$ and $\varepsilon_{a,s}$ are the lateral strain and axial strain of steel tube, $\varepsilon_{a,se}$ and $\varepsilon_{a,sp}$ are the yield strain and plastic axial strain, respectively. It should be noted that the elastic modulus of steel tube is assumed as 200 GPa and the yield strain ($\varepsilon_{a,se}$) is calculated from yield stress divided by elastic modulus which is based on an elastic-perfect plastic stress-strain model. Test results reported in [33] were used to validate the accuracy of this axial-lateral strain relationship, which will be further discussed later.

3.2 Axial and Lateral behaviour of concrete

For the concrete core in unconfined stage, which is under a uniaxial compression case, the stress-strain relationship with cylinder strengths from 12 to 90 MPa from Eurocode 2 [36] is adopted, as expressed in Eqs. 3-5:

$$\sigma_c = f_{co}\left[\frac{k\eta - \eta^2}{1+(k-2)\eta}\right] \tag{3}$$

$$k = 1.05E_c\left(\varepsilon_{co} / f_{co}\right) \tag{4}$$

$$\eta = \varepsilon_c / \varepsilon_{co} \tag{5}$$

where σ_c and ε_c are the uniaxial compressive stress and strain of concrete, f_{co} is the compressive cylinder strength of concrete, E_c is the elastic modulus of concrete and ε_{co} is the axial strain at peak stress.

The lateral strain could be obtained through a well validated axial-to-lateral strain model of concrete. There have been numerous axial strain-lateral strains models for concrete in existing literature. Teng et al. [13] firstly proposed a model which could capture the lateral strain-axial strain response of actively confined, passively confined and unconfined concrete. It is indicated

that this model is applicable for both normal strength concrete and high strength concrete. Lim and Ozbakkaloglu [37] also proposed a lateral-axial strain model for the actively and passively confined concrete, and this model was based on the experimental database of FRP confined concrete (passively confined) which covers the concrete cylinder strength from 6.2 to 169.7 MPa and the confining stress ratio (i.e. confining pressure to concrete cylinder strength ratio) ranges from 0 to 1. Recently, Kwan et al. [14] proposed a lateral-axial strain model of confined concrete which separates the relationship into two portions, before and after the formation of splitting cracks. A formula was proposed to predict the axial strain at transition points based on an experimental database of confined concrete in which the cylinder strength ranges from 25 to 112 MPa and the confining stress ratio varies from 0 to 0.99. Lai et al. [38] also proposed an axial-lateral strain relationship which considers not only the effect of confining pressure but the influence of concrete strength. The unconfined and ring-confined, spiral-confined and tie-confined CFST test results were used as the database which covers the concrete cylinder strength ranging from 27 to 125.3 MPa, and the confinement ratio, defined as the ratio of sectional capacity of steel over sectional capacity of concrete core, ranges from 0.16 to 4.22. The abovementioned four models are all proposed for the confined concrete, and these models are also applicable to the unconfined concrete where the confining pressure is zero. These four models were then assessed by existing experimental responses of the lateral behaviour of concrete (cylinders tests conducted in [33]) in unconfined stage. Figure 1 compares the predicted axial strain-lateral strain curves with the experimental results. It could be found that for concrete with cylinder strength of 38 MPa, the models from Teng et al.[13], Kwan et al. [14] and Lai et al. [38] reasonably capture the lateral behaviour from test results, whilst the model from Lim and Ozbakkaloglu [37] underestimates the lateral strain of the concrete cylinder under axial compression. However, when the concrete cylinder strength increases to 80.5 MPa, the models from Teng et al. [13], Kwan et al. [14] and Lai et al. [38] slightly overestimate the lateral strain, and when the concrete cylinder strength increases to 112.1 MPa, it is obviously that the lateral strain of concrete is overestimated by all the models. Thus, an accurate axial-lateral strain model should be developed for the high strength concrete. As the concrete is under uniaxial compression in unconfined stage, secant value of Poisson's ratio could be used to express the relationship between axial strain and lateral strain, as formulated in Eq. 6,

$$\varepsilon_{c,l} = \nu_c \varepsilon_{c,a} \tag{6}$$

where ν_c is the secant value of Poisson's ratio of concrete, $\varepsilon_{c,l}$ and $\varepsilon_{c,a}$ are the lateral strain and axial strain of concrete, respectively. For concrete, the initial Poisson's ratio ranges from 0.15 to 0.2 [18], however, when the compressive stress is approaching to the ultimate strength, the Poisson's ratio increases rapidly. Ottosen [39] proposed Eqs. 7 and 8 for the Poisson's ratio in concrete until failure:

$$\nu_c = \nu_{c,i} \qquad \text{when } \beta \leq \beta_0 \tag{7}$$

$$v_c = v_{c,f} - (v_{c,f} - v_{c,i})\sqrt{1-\left(\frac{\beta-\beta_0}{1-\beta_0}\right)^2} \qquad \text{when } \beta > \beta_0 \tag{8}$$

where $v_{c,i}$ is the Poisson's ratios at initial stage, and $v_{c,f}$ is the secant value of Poisson's ratio at peak stress. β is defined as the ratio between the current axial stress to the ultimate stress of concrete. β_0 is the stress point when the Poisson's ratio start to deviate from the initial value, $v_{c,i}$. Ottosen [39] and Candappa et al. [18] suggested a β_0 value of 0.8 for concrete cylinder strength ranging from 40 to 100 MPa which is adopted in current investigation. The initial Poisson's ratio $v_{c,i}$ is adopted from Candappa et al. [2] with a formula based on the experimental results with concrete cylinder strength ranging from 40-100 MPa which is shown as follows:

$$v_{c,i} = 8\times10^{-6}\left(f_{co}\right)^2 + 0.0002 f_{co} + 0.138 \tag{9}$$

where f_{co} is the compressive cylinder strength of concrete. For the secant value of Poisson's ratio at peak stress, Ottosen [39] suggested a $v_{c,f}$ value of 0.36, however, Candappa et al. [18] indicated that the value of 0.36 is quite low, and suggested using 0.5 instead. The Poisson's ratio at ultimate stage is significant in determining the axial strain point where the confinement starts. The concrete cylinder tests reported in [33] and some additional cylinder tests with compressive cylinder strength ranging from 37.3 MPa to 125.5 MPa were used to assess the secant value of Poisson's ratio at peak stress. In these cylinder tests, both axial and lateral strains were recorded by 60 mm strain gauges with a measuring limit of 2%. The Poisson's ratio at peak stress for each specimen is reported in Table 1 where f_{co} is the measured compressive cylinder strength of concrete, ε_{co} and $\varepsilon_{co,l}$ are the axial strain and lateral strain at peak stress, and CoV represents the coefficient of variance. It was found that the $v_{c,f}$ value suggested by Candappa et al. [18], i.e. 0.5, is suitable for those concrete cylinders with strength lower than 60 MPa. However, when the concrete cylinder strength varies from 60 to 90 MPa, the average value decreases to 0.39. For concrete with cylinder strength higher than 90 MPa the average value of $v_{c,f}$ is only about 0.28. Based on this observation and the results of compressive test on concrete standard cylinders, the following equation was proposed for the secant value of Poisson's ratio for concrete.

$$v_{c,f} = \begin{cases} 0.45 & f_{co} \le 60 \text{ MPa} \\ 0.45 - 0.00252(f_{co} - 60) & f_{co} > 60 \text{ MPa} \end{cases} \tag{10}$$

As the lateral strains of the steel tube and the concrete core are captured, the interaction point of steel and concrete can be then found. In the experimental investigations on CFSTs [33], both the CFST columns and the individual components (hollow steel tube and plain concrete columns) were tested under axial compression, and the axial and lateral strains were recorded. Thus, the axial-lateral strain relationship from each individual component was collected to investigate the interaction in CFST. Figure 2 shows the axial strain-lateral strain curves of concrete cores and steel tubes obtained from tests and predictions based on Eqs. 6-10, in which $f_{co,c}$ is the measured compressive strength of plain concrete columns and f_{co} is the compressive cylinder strength. In Figure 2, the intersection of two curves means that the lateral strain of concrete reaches the lateral strain of steel tube, where the confinement starts. It should be noted

that the end of curve of concrete means the peak load is reached. It could be found that the proposed axial strain-lateral strain models could well predict the experimental results. Figure 2 also indicates that for the circular CFST specimen with concrete cylinder strength of 38 MPa ($f_{co,c}$ = 37.1 MPa), the confining stage initiates before the peak load of the concrete (the intersection is before the peak load of concrete) however when the concrete cylinder strength increases to 80.5 MPa ($f_{co,c}$ = 71.4 MPa), the confining stage almost starts at the same time as the concrete reaches its peak load (the intersection is near the end of the concrete curve). For those concrete with cylinder strength of 112.1 MPa ($f_{co,c}$ = 100.5 MPa), the peak load is attained before the steel tube starts to confine the concrete (no intersection). In the experimental observation of the compressive test of high strength concrete, brittle failure always happened at peak stress of concrete due to a large energy release. Such brittle failure may cause a serious damage on concrete core even if the external steel tube could provide confinement immediately after peak stress of concrete. The failure mode of the CFST specimens also indicated the damage of concrete core is more serious in those CFSTs where the confinement happened after the concrete core reached its unconfined compressive strength [33].

4. Confined stage

Under confined stage, the stress-strain relationship of CFST could be divided into (1) a passively confined concrete stress-strain model and (2) a descending axial stress-strain model of steel under biaxial stresses due to the increasing lateral strain. The basic assumption in this stage is that the axial strain and lateral strain of concrete core and steel tube increases simultaneously. The following subsections describe the behaviours of the steel tube and the concrete core in CFST under the confined stage.

4.1 Axial and lateral behaviour of steel

In confined stage, the steel tube is under biaxial stress state, and the stresses in axial and lateral direction could be determined by the increment of strains in these two directions. In the incremental analysis, J_2 flow theory of plasticity [40] was used for the steel constitutive model. The stresses of steel tubes are calculated by the generalized Hooke law and incremental Prandtl-Reuss equations respectively, as expressed in following equations [40].

$$\begin{Bmatrix} d\sigma_1^i \\ d\sigma_2^i \end{Bmatrix} = \frac{E_s}{1-\nu_s}\begin{bmatrix} 1 & \nu_s \\ \nu_s & 1 \end{bmatrix}\begin{Bmatrix} d\varepsilon_1^i \\ d\varepsilon_2^i \end{Bmatrix} \quad \text{(Elastic stage)} \tag{11}$$

$$\begin{Bmatrix} d\sigma_1^i \\ d\sigma_2^i \end{Bmatrix} = \frac{E_s}{1-\nu_s}\begin{bmatrix} 1-\dfrac{S_a^{\,2}}{S_c} & \nu_s-\dfrac{S_aS_b}{S_c} \\ \nu_s-\dfrac{S_aS_b}{S_c} & 1-\dfrac{S_b^{\,2}}{S_c} \end{bmatrix}\begin{Bmatrix} d\varepsilon_1^i \\ d\varepsilon_2^i \end{Bmatrix} \quad \text{(Plastic stage)} \tag{12}$$

$$S_a = s_1 + \nu_s s_2 \tag{13}$$

$$S_b = s_2 + \nu_s s_1 \tag{14}$$

$$S_c = s_1^2 + s_2^2 + 2\nu_s s_1 s_2 \tag{15}$$

$$s_1 = \frac{1}{3}\left(2\sigma_1^{i-1} - \sigma_2^{i-1}\right) \tag{16}$$

$$s_2 = \frac{1}{3}\left(2\sigma_2^{i-1} - \sigma_1^{i-1}\right) \tag{17}$$

where σ_1 and σ_2 are the axial and the lateral stresses, respectively, ε_1 and ε_2 are the axial and the lateral strains, respectively, E_s is the Young's modulus of steel, ν_s is the Poisson's ratio of steel, and i presents the increment number. Eq. 11 is for the elastic stage of steel and Eq. 12 is for the plastic stage. The von Mises yield surface was used to identify whether the material yields or not.

$$\left(\sigma_1^{i-1}\right)^2 + \left(\sigma_2^{i-1}\right)^2 - \left(\sigma_1^{i-1}\sigma_2^{i-1}\right) - f_y^{\,2} = 0 \tag{18}$$

In this incremental analysis, the compressive stress and strain in axial direction are defined as positive and the tensile stress and strain in lateral direction are defined as negative. The lateral strain to lateral stress relationship in the steel tube now could be developed and used in the passive-confinement model in CFST.

4.2 Axial and lateral behaviour of concrete

As mentioned before, in confined stage, concrete is passively confined under triaxial stress state. Teng et al. [13] indicated that in passive-confinement model of concrete, under the same confining pressure, the axial stress and strain are identical to that in active-confinement model with constant confining pressure. In other words, the loading path is independent on the stress-strain relationship of passively confined concrete. Teng et al. [13] suggested that a step-by-step incremental process could be developed for the stress–strain curve of passively confined concrete by using a series of stress–strain curves from actively confined concrete with different confining pressures. Thus, a passive-confinement model could be derived from the following relationships: (i) a well-developed active-confinement stress-strain model, (ii) a relationship between lateral strain of confined concrete to its confining pressure and (iii) a lateral strain to axial strain model of confined concrete under confining pressure.

The stress-strain equation of active-confinement model used in this investigation is firstly proposed by Popovics [15] and then adopted in Mander et al. [8] in steel confined concrete model:

$$\frac{\sigma_c}{f_{cc}} = \frac{\left(\varepsilon_c / \varepsilon_{cc}\right) r}{r - 1 + \left(\varepsilon_c / \varepsilon_{cc}\right)^r} \tag{19}$$

$$r = \frac{E_c}{E_c - f_{cc}/\varepsilon_{cc}} \tag{20}$$

where f_{cc} is the compressive strength of confined concrete and ε_{cc} is the axial strain of confined

concrete at peak stress. The ultimate stress of confined concrete and the corresponding strain have been investigated by many researchers [8, 16, 18, 30, 32]. In current investigation, the following equations from Jiang and Teng [32] were adopted for those concrete with cylinder strength lower than 60 MPa.

$$\frac{f_{cc}}{f_{co}} = 1 + 3.5\frac{f_l}{f_{co}} \tag{21}$$

$$\frac{\varepsilon_{cc}}{\varepsilon_{co}} = 1 + 17.5\left(\frac{f_l}{f_{co}}\right)^{1.2} \tag{22}$$

where f_l is the confining pressure. For the high strength concrete, Xiao et al. [30] updated the peak stress and corresponding strain of confined high strength concrete and the following equations were adopted for the CFST with high strength concrete with cylinder strength higher than 60 MPa:

$$\frac{f_{cc}}{f_{co}} = 1 + 3.24\left(\frac{f_l}{f_{co}}\right)^{0.8} \tag{23}$$

$$\frac{\varepsilon_{cc}}{\varepsilon_{co}} = 1 + 17.5\left(\frac{f_l}{f_{co}}\right)^{1.06} \tag{24}$$

To implement the incremental process of the analytical model, the relationship of confining pressure to the lateral strain of confined concrete should be well understood. It is clear that the passive confining pressure is related to the lateral stress in the external confining jacket. With circular section, the confining pressure and lateral stress has the following relationship:

$$f_l = \frac{2\sigma_l t}{D - 2t} \tag{25}$$

where σ_l is the lateral stress in external confining jacket such as FRP or steel tube, t is the thickness of the jacket, and D is the external diameter of column. In FRP confined concrete, the relationship of lateral stress and lateral strain is linear. However, in CFST, the steel tube is under biaxial stress state, so the lateral stress in steel tube, $\sigma_{s,l}$, is related to the both axial strain and lateral strain. The following relationship in the incremental process exists and Eqs. 11 and 12 were adopted for this function:

$$d\sigma_{s,l} = f\left(d\varepsilon_{s,a},\ d\varepsilon_{s,l}\right) \tag{26}$$

The final required relationship, the lateral strain to axial strain relationship of confined concrete, was adopted from Teng et al. [13]. The equation is shown as follows:

$$\frac{\varepsilon_c}{\varepsilon_{co}} \Big/ \left(1 + 8\frac{f_l}{f_{co}}\right) = 0.85\left\{\left[1 + 0.75\left(\frac{-\varepsilon_{c,l}}{\varepsilon_{co}}\right)\right]^{0.7} - \exp\left[-7\left(\frac{-\varepsilon_{c,l}}{\varepsilon_{co}}\right)\right]\right\} \tag{27}$$

where f_l is the confining pressure; $\varepsilon_{c,l}$ is the lateral strain of the concrete core. Teng et al. [13] indicated that this equation is applicable for both normal strength concrete and high strength concrete under confinement. Using Eqs. 19-27, the stress-strain relationship of confined

concrete core in CFST could be established.

5. Analytical model of CFST

Based on the abovementioned stages of CFST under uniaxial compression and the stress-strain relationship of each component (concrete core and steel tube). An analytical model for CFST is proposed in this investigation through an iteration process to capture a confining pressure related stress-strain model of CFST stub columns.

5.1 Implementation of analytical model

A sub-routine was written to implement the incremental process of the analytical model of CFST. The whole analysis process is illustrated in a flow chat as shown in Figure 3 and each step of the analytical model is detailed as follows:

Step 1, Unconfined stage:

Firstly, an increment in axial strain ($d\varepsilon_a$) of both steel and concrete is given. Eqs. 1-5 and were used to update the axial stresses of concrete ($\sigma_{c,a}$) and steel ($\sigma_{s,a}$), respectively. Then the yield condition of steel is checked based on the von Mises yield function and the lateral strain of steel tube ($\varepsilon_{s,l}$) is calculated by Eq. 1 (before yielding) or Eq. 2 (after yielding). Meanwhile, Eqs. 6-10 were used to calculate the Poisson's ratio of concrete and the lateral strain of concrete ($\varepsilon_{c,l}$). Finally, the lateral strain of concrete is checked if it is larger than the lateral strain of steel tube. The incremental process continues until the lateral strain of concrete is equal or larger than that of steel tube.

Step 2, Confinement initiates:

Then the $d\varepsilon_a$ in current step is adjusted to converge $\varepsilon_{s,l}$ and $\varepsilon_{c,l}$ with error less than 0.1%. In the subsequent incremental process $\varepsilon_{s,l}$ and $\varepsilon_{c,l}$ increase simultaneously.

Step 3, Confining stage:

In confining stage, the axial strains and lateral strains of concrete core and steel tube are increasing simultaneously. Firstly, an increment in lateral strain ($d\varepsilon_l$) is given and a value of confining pressure (f_l') is assumed. Then Eq. 27 is used to calculate the current axial strain of concrete core. And the increment of axial strain ($d\varepsilon_a$) and lateral strain ($d\varepsilon_l$) are used to determine the axial stress ($\sigma_{s,a}$) and lateral stress ($\sigma_{s,l}$) of steel tube using Eqs. 11-18. Then the lateral stress of steel is used to determine the confining pressure (f_l) via Eq. 25. If the calculated confining pressure f_l is not equal to the assumed confining pressure f_l', then update the assumed f_l' and calculate a new confining pressure until f_l is equal to f_l'. And then the calculated f_l and axial strain ε_a are used to calculate the axial stress of confined concrete using Eqs. 19-24. Finally, the determined axial stress of confined concrete $\sigma_{c,a}$ and the axial stress of steel tube from the J_2 flow theory $\sigma_{s,a}$ together with the cross-sectional areas are used to calculate the axial bearing load of CFST.

5.2 Effective confining pressure for high strength concrete

It was observed that high strength concrete has a brittle failure at peak stress which may result

in a premature damage of concrete before the confinement starts. The recorded lateral strains from strain gauges at different locations of mid-height of the specimens 30C-1, 50C-1 and 80C-1 in Zhu and Chan [33] are presented in Figure 4. It can be found that for specimens 50C-1 and 80C-1, the readings of strain gauges from each location differ after the unconfined concrete reaches its peak load where the confining stage starts (illustrated in Figure 2b and 2c), however, this phenomenon is minor in specimen 30C-1 whose concrete core could be confined before its peak stress. This observation indicated that the damage of local failure in high strength concrete core results in a non-uniformly confinement in the circular CFST and may affect its behaviour after confinement. Experimental data of high strength CFST with concrete cylinder strength larger than 60 MPa in Zhu and Chan [33] and results from Han et al. [41] where both load capacity and corresponding axial deformation are available were collected to assess this effect on load capacity and the axial deformation at peak load of CFST. Table 2 lists the collected experimental data, in which D is the external diameter of the steel tube, t is the wall thickness of the steel tube, and ε_u is the strain at ultimate load. Figure 5 shows the comparison of the analytical model and experimental results. It could be found that the load capacity of the CFST specimens could be captured but the model overestimates the axial deformation significantly. This is caused by the above-mentioned premature local damage in high strength concrete core and non-uniform confinement. Therefore, a reduction factor k_1 was proposed to the equation of confining pressure to account for the reduction of confining pressure in high strength concrete.

$$f_l = k_1 \frac{2\sigma_l t}{D-2t} \tag{28}$$

where

$$k_1 = \begin{cases} 1 & f_{co} \le 50 \text{ MPa} \\ \dfrac{50}{f_{co}} & f_{co} > 50 \text{ MPa} \end{cases} \tag{29}$$

Figure 5 presents the comparison of the analytical model with the effective confining pressure with the test results and accurate prediction could be obtained in both load capacity and the corresponding deformation.

6. Assessment of model

In the assessment of the analytical model, the axial load capacity, the load-axial deformation response and lateral-axial strain relationship of CFST with circular section were examined. In the assessment of load capacity, a test database consisting of 597 specimens collected from existing literature was used [2, 6, 11, 42-85]. The database covers the concrete cylinder strength from 13.3-184.4 MPa and steel yield stress from 186-853 MPa. The validation of load bearing capacity is shown in Figure 6 and Table 2. The mean value of the $N_{u,model}/N_{u,test}$ of the 597 circular CFST specimens is 0.99 and the corresponding coefficient of variance (CoV) is 0.13, in which $N_{u,model}$ is the predicted axial load capacity using the proposed analytical model and $N_{u,test}$ is the experimental load capacity. In the assessment of load-axial deformation response, as there are limited information available from literature, in this research, 2 test results from Han and Yao [84], 2 test results from Sakino et al. [11] and test results from Zhu and Chan [33]

investigation were used for the validation. Figure 7 depicts the assessment of load-axial shortening relationship of CFST. It could be found that the analytical model from Kwan et al. [14] overestimates the test results of CFST with high strength concrete, the current model can replicate the load-strain history of CFST precisely for both hardening behaviour and softening behaviour. This analytical model also could capture the lateral-axial strain response on steel tube in CFST. Due to limited test results of lateral strain available from existing literature, the recorded lateral-axial strain relationship in Zhu and Chan [33], Lai et al. [86] and Lin et al. [87] were used to assess the accuracy of the analytical model. Figure 8 shows the prediction of axial-lateral strain response on steel tube. The proposed model and the model from Kwan et al. [14] yields accurate predictions on lateral behaviour of CFST with normal strength concrete (Figure 8a, 8d, 8e, 8g and 8h), however the model from Kwan et al. [14] slightly underestimates the lateral strain in CFST with high strength concrete (Figure 8b). The proposed model can well capture the lateral behaviour in the specimens with concrete cylinder strength of 38 MPa and 89.9 MPa, but only satisfactory for specimens with concrete cylinder strength of 112.1 MPa in which brittle failure and non-uniform confinement lead to an inconsistent lateral behaviour as evidenced in Figure 8c, the curves from repeated specimens 80C-1, 80C-2 and 80C-3 deviate from each other.

7. Assumptions and Limitations

The proposed analytical model for CFST is established based on material constitutive models and interaction behaviour between concrete and steel tube, which considers the distinct lateral behaviour of high strength concrete and an effective confining pressure because of non-uniform confinement due to the premature failure of concrete core. However, there are some assumptions and limitations that should be stated which are summarised as follows:

1. At the initial stage of loading, the model assumes there is no interaction between concrete and steel tube, which neglects the initial bonding stress between concrete and steel tube. However, the bonding stress may affect the lateral behaviour of steel tube and concrete core. The dilation of steel tube is larger than concrete, therefore the bonding stress may restrain the expansion of the steel tube. A previous study [88] shows that the initial bonding stress has minor influence on the confining stress-axial strain relationship of CFST with high strength concrete at initial stage of loading. Thus, the interfacial bonding stress at initial stage is not considered in this model.
2. The analytical model assumes the stress-strain behaviour of passive confined concrete is stress-path independent. However, investigations [30, 89, 90] have mentioned that the path independence assumption may deviate from the actual behaviour of passively confined concrete with high strength concrete. The axial stress in passively confined concrete is lower than that in actively confined concrete due to the concrete stiffness and development of concrete microcracks. Further investigations are needed to evaluate the effect of stress-path dependence on the stress-strain behaviour of confined concrete in CFST.
3. The analytical model has not considered the buckling behaviour of the steel tube. The local buckling behaviour of steel tube in CFST is restrained by the existence of inner concrete core, thus the buckling theory for hollow steel tube is not applicable. In this study, a

conservative limit based on the Eurocode 3 [91] of $D/t<90(235/f_y)$ for steel tube is suggested to avoid any local buckling of steel tube. Further investigations on the local buckling behaviour of thin steel tubes in CFSTs are needed.

8. Conclusions

This paper presents an analytical model of CFST with a strain incremental process. The key contributions of this analytical model are summarized as follows:

1. The model captures the initiation of confinement in CFSTs and the distinct lateral behaviour of high strength concrete is considered
2. A strain incremental process with an iteration process based on the constitutive model of the passively confined concrete and the biaxially-stressed steel tube was proposed to predict both the axial and lateral behaviour of CFST stub columns.
3. An effective confining pressure with a reduction factor is applied to the CFST to consider the non-uniform confinement for the high strength concrete.
4. The proposed model was validated by 597 existing experimental data and the results show that the analytical model could capture the load capacity of circular CFST and also well predict the axial load-strain relationship as well as the lateral-axial strain relationship.
5. The analytical model could be used to establish a confining pressure-related constitutive model for the confined concrete in CFST and contributes to future numerical investigations such as finite element modelling of CFST.

Acknowledgement

The authors appreciate the support from the Chinese National Engineering Research Centre for Steel Construction (Hong Kong Branch) at The Hong Kong Polytechnic University.

References

[1] Furlong RW. Strength of steel-encased concrete beam columns. Journal of the Structural division. 1967;93:113-24.
[2] Giakoumelis G, Lam D. Axial capacity of circular concrete-filled tube columns. Journal of Constructional Steel Research. 2004;60:1049-68.
[3] Kloppel V.K. G, W. An investigation of the load carrying capacity of concrete-filled steel tubes and development of design formula. Der Stahlbau. 1957;26:44-50.
[4] Liew J, Xiong D. Experimental investigation on tubular columns infilled with ultra-high strength concrete. Tubular Structures XIII-Proceedings of the 13th International Symposium on Tubular Structures2010. p. 637-45.
[5] O'Shea MD, Bridge RQ. Design of circular thin-walled concrete filled steel tubes. Journal of Structural Engineering. 2000;126:1295-303.
[6] Schneider SP. Axially loaded concrete-filled steel tubes. Journal of structural Engineering. 1998;124:1125-38.
[7] Tomii M. Experimental studies on concrete filled steel tubular stub columns under

453 concentric loading. Proceedings of International Colloquium on Stability of Structures Under
454 Static and Dynamic Loads, SSRC/ASCE/Washington, DC1977.
455 [8] Mander JB, Priestley MJ, Park R. Theoretical stress-strain model for confined concrete.
456 Journal of structural engineering. 1988;114:1804-26.
457 [9] Richart FE, Brandtzaeg A, Brown RL. A study of the failure of concrete under combined
458 compressive stresses. University of Illinois at Urbana Champaign, College of Engineering …;
459 1928.
460 [10] Johansson M, Gylltoft K. Mechanical behavior of circular steel–concrete composite stub
461 columns. Journal of structural engineering. 2002;128:1073-81.
462 [11] Sakino K, Nakahara H, Morino S, Nishiyama I. Behavior of centrally loaded concrete-
463 filled steel-tube short columns. Journal of structural engineering. 2004;130:180-8.
464 [12] Mirmiran A, Shahawy M. A new concrete-filled hollow FRP composite column.
465 Composites Part B: Engineering. 1996;27:263-8.
466 [13] Teng J, Huang Y, Lam L, Ye L. Theoretical model for fiber-reinforced polymer-confined
467 concrete. Journal of composites for construction. 2007;11:201-10.
468 [14] Kwan A, Dong C, Ho J. Axial and lateral stress–strain model for circular concrete-filled
469 steel tubes with external steel confinement. Engineering Structures. 2016;117:528-41.
470 [15] Popovics S. A numerical approach to the complete stress-strain curve of concrete. Cement
471 concrete research. 1973;3:583-99.
472 [16] Attard MM, Setunge S. Stress-strain relationship of confined and unconfined concrete.
473 Materials Journal. 1996;93:432-42.
474 [17] Binici B. An analytical model for stress–strain behavior of confined concrete. Engineering
475 structures. 2005;27:1040-51.
476 [18] Candappa D, Sanjayan J, Setunge S. Complete triaxial stress-strain curves of high-strength
477 concrete. Journal of Materials in Civil Engineering. 2001;13:209-15.
478 [19] Ellobody E, Young B, Lam D. Behaviour of normal and high strength concrete-filled
479 compact steel tube circular stub columns. Journal of Constructional Steel Research.
480 2006;62:706-15.
481 [20] Fam AZ, Rizkalla SH. Confinement model for axially loaded concrete confined by circular
482 fiber-reinforced polymer tubes. Structural Journal. 2001;98:451-61.
483 [21] Harries KA, Kharel G. Behavior and modeling of concrete subject to variable confining
484 pressure. Materials Journal. 2002;99:180-9.
485 [22] Liang QQ, Fragomeni S. Nonlinear analysis of circular concrete-filled steel tubular short
486 columns under axial loading. Journal of Constructional Steel Research. 2009;65:2186-96.
487 [23] Lu X, Hsu C-TT. Behavior of high strength concrete with and without steel fiber
488 reinforcement in triaxial compression. Cement Concrete Research. 2006;36:1679-85.
489 [24] Mirmiran A, Shahawy M. Behavior of concrete columns confined by fiber composites.
490 Journal of structural engineering. 1997;123:583-90.
491 [25] Pramono E, Willam K. Fracture energy-based plasticity formulation of plain concrete.
492 Journal of Engineering Mechanics. 1989;115:1183-204.
493 [26] Razvi S, Saatcioglu M. Confinement model for high-strength concrete. Journal of
494 Structural Engineering. 1999;125:281-9.

[27] Spoelstra MR, Monti G. FRP-confined concrete model. 1999;3:143-50.
[28] Thai H-T, Uy B, Khan M, Tao Z, Mashiri F. Numerical modelling of concrete-filled steel box columns incorporating high strength materials. Journal of Constructional Steel Research. 2014;102:256-65.
[29] Willam KJ. Constitutive model for the triaxial behaviour of concrete. Proc Intl Assoc Bridge Structl Engrs. 1975;19:1-30.
[30] Xiao Q, Teng J, Yu T. Behavior and modeling of confined high-strength concrete. Journal of Composites for Construction. 2010;14:249-59.
[31] Xie J, Elwi A, MacGregor J. Mechanical properties of three high-strength concretes containing silica fume. Materials Journal. 1995;92:135-45.
[32] Jiang T, Teng J. Analysis-oriented stress–strain models for FRP–confined concrete. Engineering Structures. 2007;29:2968-86.
[33] Zhu J-Y, Chan T-M. Experimental investigation on octagonal concrete filled steel stub columns under uniaxial compression. Journal of Constructional Steel Research. 2018;147:457-67.
[34] Clark W. Axial load capacity of circular steel tube columns filled with high strength concrete: Victoria University of Technology; 1994.
[35] Marin J. Mechanical behavior of engineering materials: Prentice-Hall; 1962.
[36] CEN. EN 1992-1-1, Eurocode 2 – Design of concrete structures–Part 1-1: General rules and rules for buildings. Brussels: European Committee for Standardization 2004.
[37] Lim JC, Ozbakkaloglu TJJoCfC. Confinement model for FRP-confined high-strength concrete. 2014;18:04013058.
[38] Lai MH, Ho JCM. An analysis-based model for axially loaded circular CFST columns. Thin-Walled Structures. 2017;119:770-81.
[39] Ottosen NS. Constitutive model for short-time loading of concrete. Journal of the Engineering Mechanics Division ASCE. 1979;105:127-41.
[40] Calladine CR. Plasticity for engineers: Ellis Horwood. Chichester; 1985.
[41] Han L-H, Yao G-H, Zhao X-L. Tests and calculations for hollow structural steel (HSS) stub columns filled with self-consolidating concrete (SCC). Journal of Constructional Steel Research. 2005;61:1241-69.
[42] Abed F, AlHamaydeh M, Abdalla S. Experimental and numerical investigations of the compressive behavior of concrete filled steel tubes (CFSTs). Journal of Constructional Steel Research. 2013;80:429-39.
[43] Aslani F, Uy B, Hur J, Carino P. Behaviour and design of hollow and concrete-filled spiral welded steel tube columns subjected to axial compression. Journal of Constructional Steel Research. 2017;128:261-88.
[44] Beck AT, de Oliveira WLA, De Nardim S, ElDebs ALHC. Reliability-based evaluation of design code provisions for circular concrete-filled steel columns. Engineering Structures. 2009;31:2299-308.
[45] Chan T-M, Huai Y-M, Wang W. Experimental investigation on lightweight concrete-filled cold-formed elliptical hollow section stub columns. Journal of Constructional Steel Research. 2015;115:434-44.

[46] Ding F-x, Liu J, Liu X-m, Yu Z-w, Li D-w. Mechanical behavior of circular and square concrete filled steel tube stub columns under local compression. Thin-Walled Structures. 2015;94:155-66.
[47] Duarte APC, Silva BA, Silvestre N, De Brito J, Júlio E, Castro JM. Tests and design of short steel tubes filled with rubberised concrete. Engineering Structures. 2016;112:274-86.
[48] Ekmekyapar T, Al-Eliwi BJM. Experimental behaviour of circular concrete filled steel tube columns and design specifications. Thin-Walled Structures. 2016;105:220-30.
[49] Ekmekyapar T, Al-Eliwi BJM. Concrete filled double circular steel tube (CFDCST) stub columns. Engineering Structures. 2017;135:68-80.
[50] Evirgen B, Tuncan A, Taskin K. Structural behavior of concrete filled steel tubular sections (CFT/CFSt) under axial compression. Thin-Walled Structures. 2014;80:46-56.
[51] Gupta PK, Sarda SM, Kumar MS. Experimental and computational study of concrete filled steel tubular columns under axial loads. Journal of Constructional Steel Research. 2007;63:182-93.
[52] Han L-H, Liu W, Yang Y-F. Behaviour of concrete-filled steel tubular stub columns subjected to axially local compression. Journal of Constructional Steel Research. 2008;64:377-87.
[53] Han L-H, Yao G-H, Chen Z-B, Yu Q. Experimental behaviours of steel tube confined concrete (STCC) columns. Steel and Composite Structures. 2005;5:459-84.
[54] He L, Zhao Y, Lin S. Experimental study on axially compressed circular CFST columns with improved confinement effect. Journal of Constructional Steel Research. 2018;140:74-81.
[55] Huang M, Li B, Wen Y. Analysis on the Influence of Restraining Effect Coefficient on the Mechanical Property of the Concrete-filled Steel Tube. JOURNAL-CHONGQING JIANZHU UNIVERSITY. 2008;30:90.
[56] Kang H-S, Lim S-H, Moon T-S, Stiemer SF. Experimental study on the behavior of CFT stub columns filled with PCC subject to concentric compressive loads. Steel and Composite Structures. 2005;5:17-34.
[57] Kato B. Compressive strength and deformation capacity of concrete-filled tubular stub columns (Strength and rotation capacity of concrete-filled tubular columns, Part 1). Journal of Structural and Construction Engineering, AIJ. 1995;468:183-91.
[58] Kilpatrick AE. The behaviour of high-strength composite concrete columns: School of Civil Engineering, Curtin University of Technology; 1996.
[59] Lai MH, Ho JCM. Effect of continuous spirals on uni-axial strength and ductility of CFST columns. Journal of Constructional Steel Research. 2015;104:235-49.
[60] Liu F, Wang Y, Chan T-m. Behaviour of concrete-filled cold-formed elliptical hollow sections with varying aspect ratios. Thin-Walled Structures. 2017;110:47-61.
[61] Lu Y, Chen J, Li S. Experimental research on steel fiber reinforced high strength concrete filled steel tubular short columns subjected to axial compression load. Jianzhu Jiegou Xuebao(Journal of Building Structures). 2011;32:166-72.
[62] Lu Y, Li N, Li S, Liang H. Behavior of steel fiber reinforced concrete-filled steel tube columns under axial compression. Construction and Building Materials. 2015;95:74-85.
[63] Miyaki S, Matsui C, Tsuda K, Hatato T, Imamura T. Axial compression behacior of

centrifugal concrete filled steel tubular columns using super high strength concrete. Journal of Structural and Construction Engineering AIJ. 1996;482:121-30.
[64] Prion HGL, Boehme J. Beam-column behaviour of steel tubes filled with high strength concrete. Canadian journal of civil engineering. 1994;21:207-18.
[65] Ren Q-X, Han L-H, Lam D, Hou C. Experiments on special-shaped CFST stub columns under axial compression. Journal of Constructional Steel Research. 2014;98:123-33.
[66] Suzuki T, Motoyui S, Ohta H. Study on structural properties of concrete silled circular steel tubular Stub columns under pure axial compression. Journal of Structural and Construction Engineering, AIJ. 1997;449:123-39.
[67] Tao Z, Han L-H, Zhao X-L. Behaviour of concrete-filled double skin (CHS inner and CHS outer) steel tubular stub columns and beam-columns. Journal of Constructional steel research. 2004;60:1129-58.
[68] Thayalan P, Aly T, Patnaikuni I. Behaviour of concrete-filled steel tubes under static and variable repeated loading. Journal of Constructional Steel Research. 2009;65:900-8.
[69] Uenaka K. CFDST stub columns having outer circular and inner square sections under compression. Journal of Constructional steel research. 2016;120:1-7.
[70] Uenaka K, Kitoh H, Sonoda K. Experimental study on short concrete filled double steel tubular columns under compression. Kou kouzou rombunshuu. 2007;14:67-75.
[71] Wang L, J.R. Q. Experimental tests on high strength concrete filled steel tube under axial compression. Building structure. 2003;33.
[72] Wang Y, Chen J, Geng Y. Testing and analysis of axially loaded normal-strength recycled aggregate concrete filled steel tubular stub columns. Engineering Structures. 2015;86:192-212.
[73] Wang Y, Chen P, Liu C, Zhang Y. Size effect of circular concrete-filled steel tubular short columns subjected to axial compression. Thin-Walled Structures. 2017;120:397-407.
[74] Wei J, Luo X, Lai Z, Varma AH. Experimental Behavior and Design of High-Strength Circular Concrete-Filled Steel Tube Short Columns. Journal of Structural Engineering. 2020;146:04019184.
[75] Xiamuxi A, Hasegawa A. Compression test of RCFT columns with thin-walled steel tube and high strength concrete. Steel and composite Structures. 2011;11:391-402.
[76] Xiong M-X, Xiong D-X, Liew JYR. Axial performance of short concrete filled steel tubes with high-and ultra-high-strength materials. Engineering Structures. 2017;136:494-510.
[77] Yang Y-F, Han L-H. Compressive and flexural behaviour of recycled aggregate concrete filled steel tubes (RACFST) under short-term loadings. Steel and Composite Structures. 2006;6:257.
[78] Yu Q, Tao Z, Wu Y-X. Experimental behaviour of high performance concrete-filled steel tubular columns. Thin-Walled Structures. 2008;46:362-70.
[79] Yu Z, Ding F, Lin S. Researches on behavior of high-performance concrete filled tubular steel short columns. Journal of Building structures. 2002;2.
[80] Yu Z-w, Ding F-x, Cai CS. Experimental behavior of circular concrete-filled steel tube stub columns. Journal of constructional steel research. 2007;63:165-74.
[81] Zhang S-m, Wang Y-y. Failure modes of short columns of high-strength concrete filled steel tubes. China Civil Engineering Journal. 2004;37:1-10.

621 [82] Zhou S, Sun Q, Wu X. Impact of D/t ratio on circular concrete-filled high-strength steel
622 tubular stub columns under axial compression. Thin-Walled Structures. 2018;132:461-74.
623 [83] Zhou X, Mou T, Tang H, Fan B. Experimental study on ultrahigh strength concrete filled
624 steel tube short columns under axial load. Advances in Materials Science and Engineering.
625 2017;2017.
626 [84] Han L-H, Yao G-H. Experimental behaviour of thin-walled hollow structural steel (HSS)
627 columns filled with self-consolidating concrete (SCC). Thin-Walled Structures. 2004;42:1357-
628 77.
629 [85] Han LH. Concrete filled steel tubular structures - theory and practice. (3rd edition). Beijing:
630 Science Press; 2016.
631 [86] Lai MH, Ho JCM. A theoretical axial stress-strain model for circular concrete-filled-steel-
632 tube columns. Engineering Structures. 2016;125:124-43.
633 [87] Lin S, Zhao Y-G, He L. Stress paths of confined concrete in axially loaded circular
634 concrete-filled steel tube stub columns. Engineering Structures. 2018;173:1019-28.
635 [88] Lai MH, Song W, Ou XL, Chen MT, Wang Q, Ho JCM. A path dependent stress-strain
636 model for concrete-filled-steel-tube column. Engineering Structures. 2020;211:110312.
637 [89] Ho JCM, Ou XL, Chen MT, Wang Q, Lai MH. A path dependent constitutive model for
638 CFFT column. Engineering Structures. 2020;210:110367.
639 [90] Lai MH, Liang YW, Wang Q, Ren FM, Chen MT, Ho JCM. A stress-path dependent stress-
640 strain model for FRP-confined concrete. Engineering Structures. 2020;203:109824.
641 [91] CEN. EN 1993-1-1, Eurocode 3-Design of steel structures, part 1-1: general rules and
642 rules for buildings. Brussels: European Committee for Standardization; 2005.
643

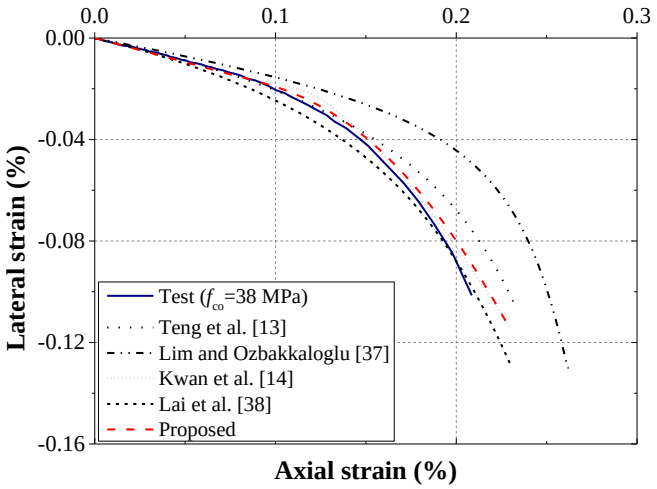

(a) Zhu and Chan [33], 38 MPa

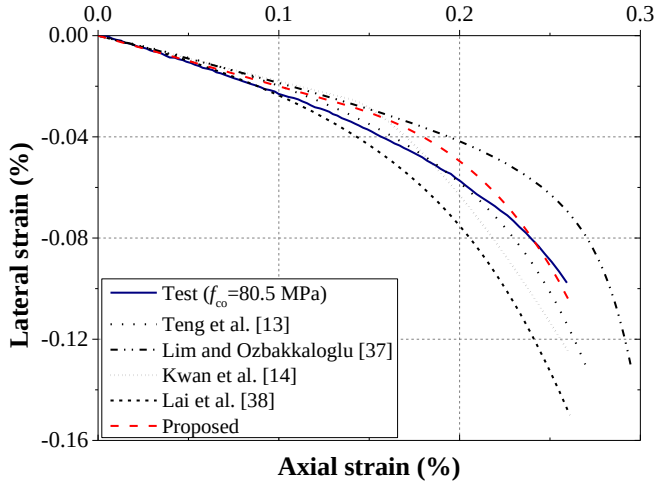

(b) Zhu and Chan [33], 80.5 MPa

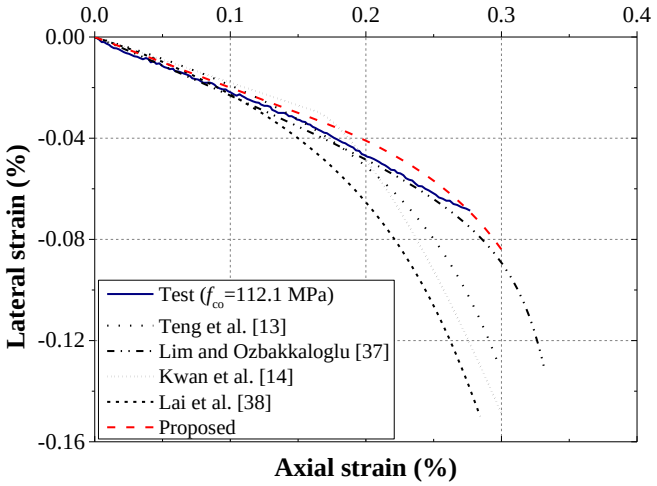

(c) Zhu and Chan [33], 112.1 MPa

Figure 1. Validation of lateral behaviour of unconfined concrete.

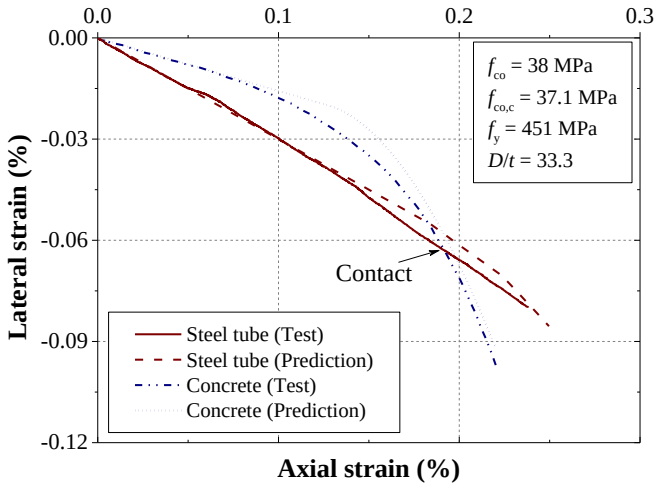

(a) Zhu and Chan [33], 30C-1

(b)

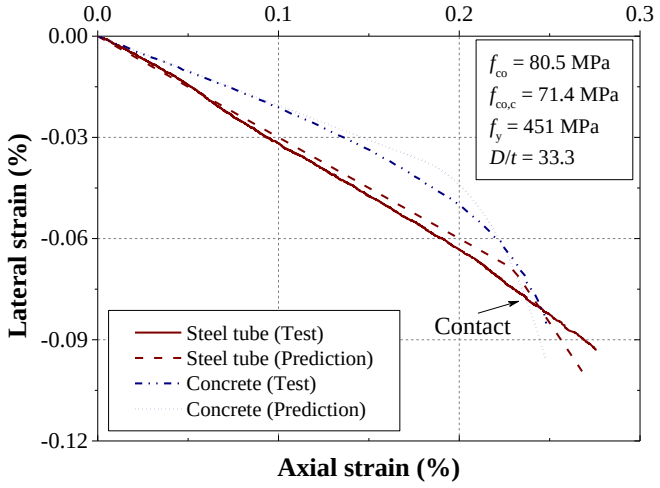

(b) Zhu and Chan [33], 50C-1

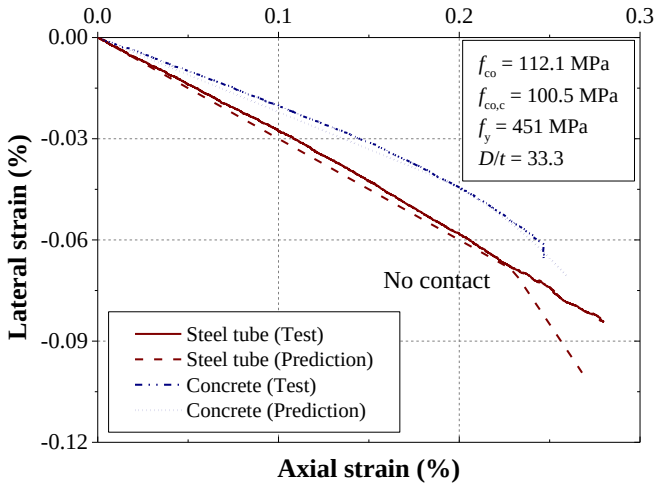

(c) Zhu and Chan [33], 80C-1

Figure 2. Test results of axial-lateral strain curves of steel and concrete.

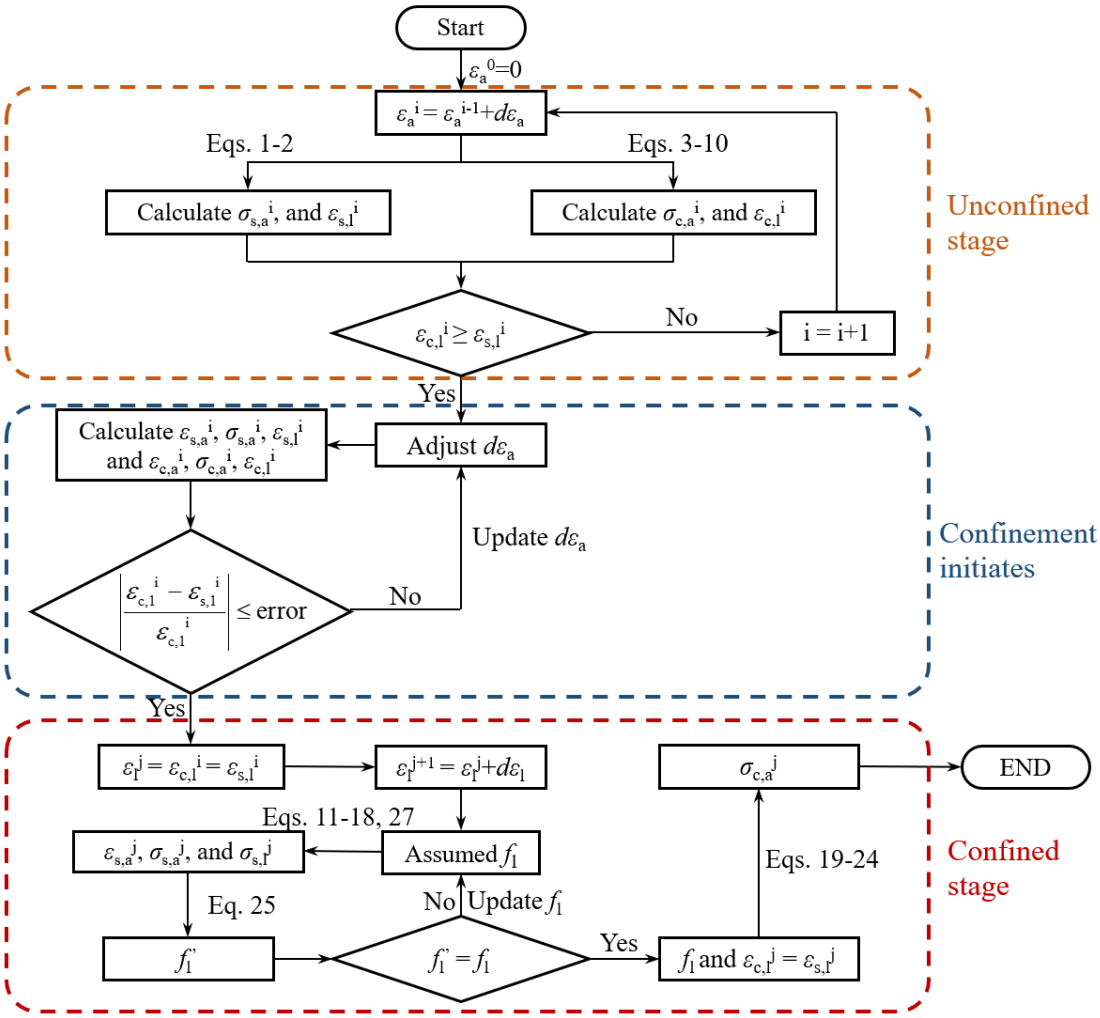

Figure 3. Flow chart of analytical model.

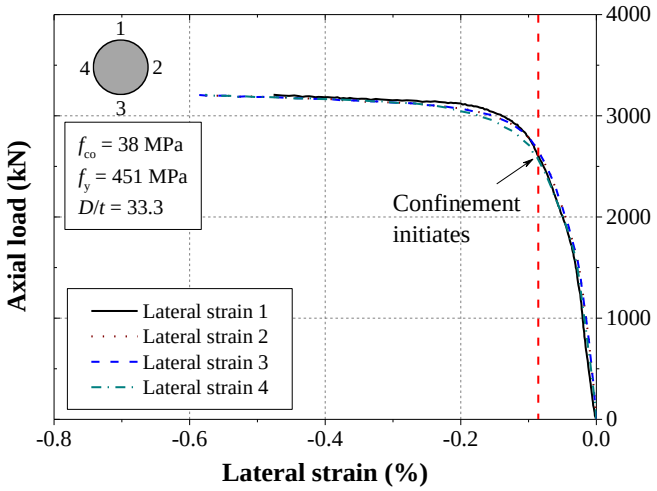

(a) Zhu and Chan [33], 30C-1

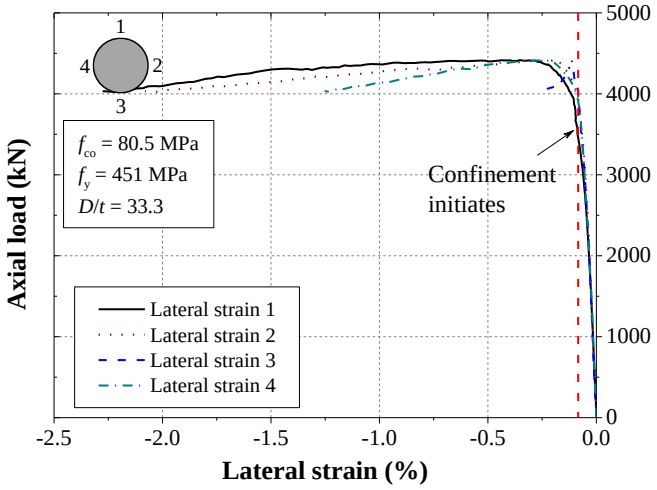

(b) Zhu and Chan [33], 50C-1

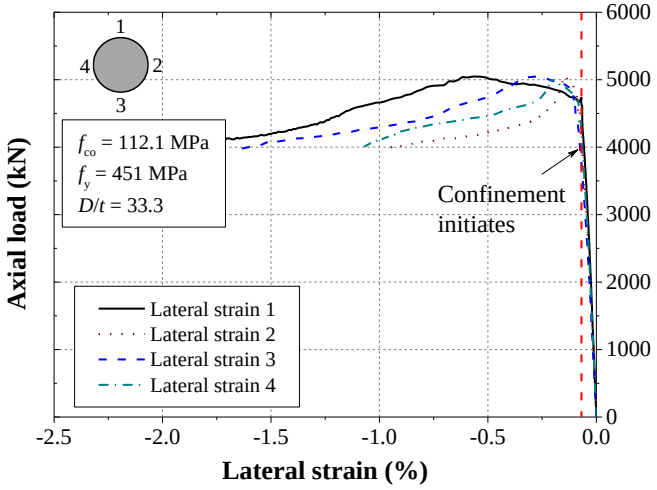

(c) Zhu and Chan [33], 80C-1

Figure 4. Lateral strain distribution in CFST with different concrete grade.

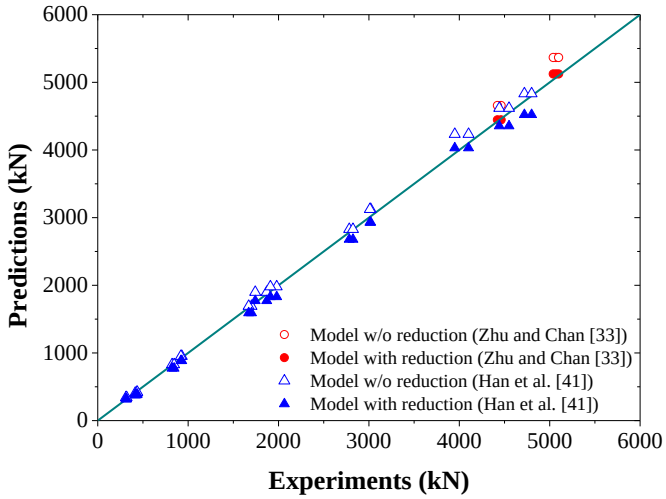

(a) Load capacity

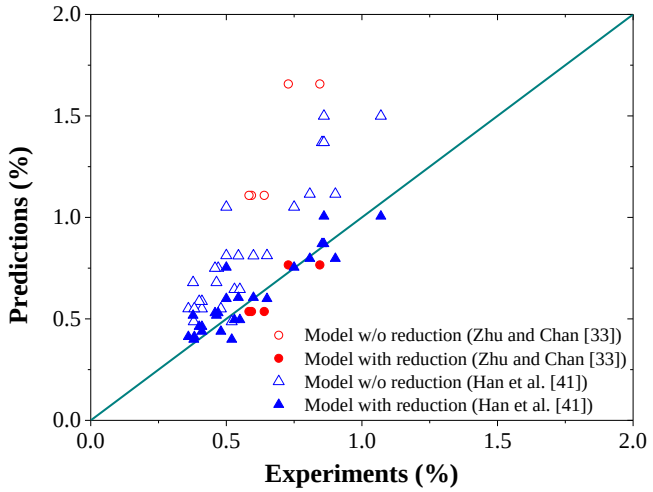

(b) Strain at peak load

Figure 5. Comparison of analytical model and experimental data of high strength concrete filled steel tubes.

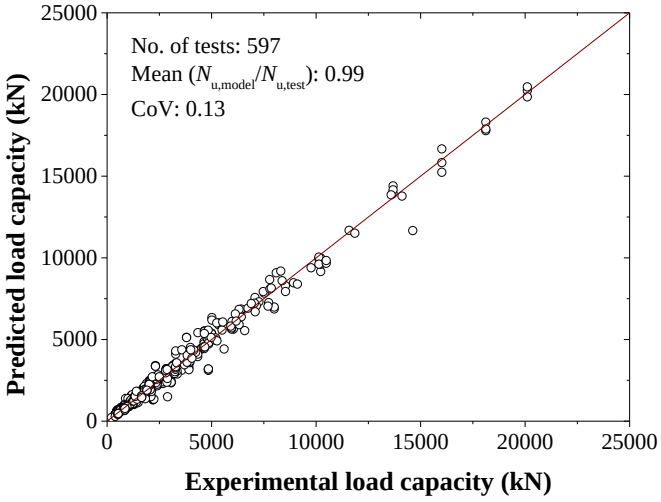

Figure 6. Assessment of load capacity of analytical model.

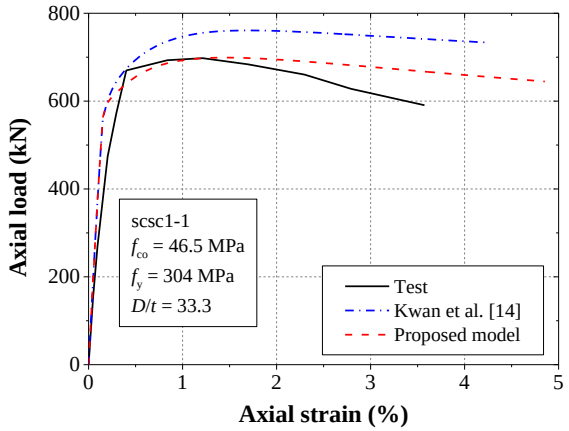

(a) Han and Yao [84], scsc1-1

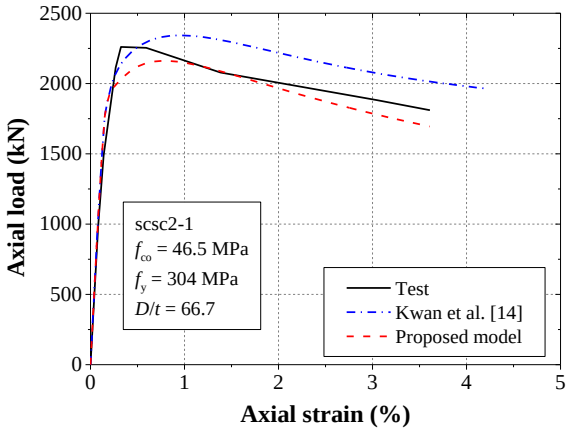

(b) Han and Yao [84], scsc1-1

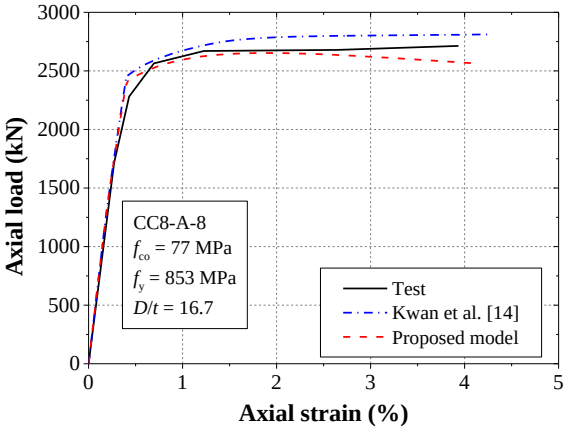

(c) Sakino et al. [11], CC8-A-8

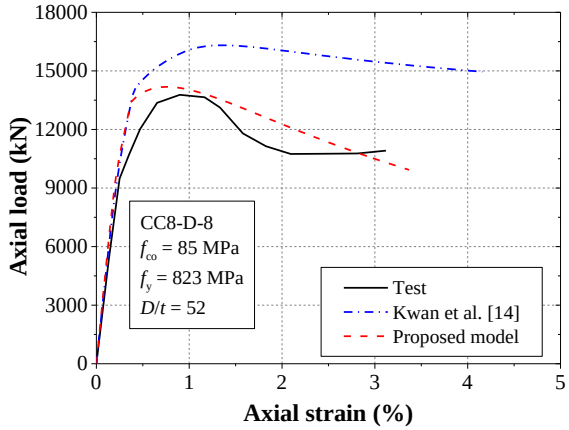

(d) Sakino et al. [11], CC8-D-8

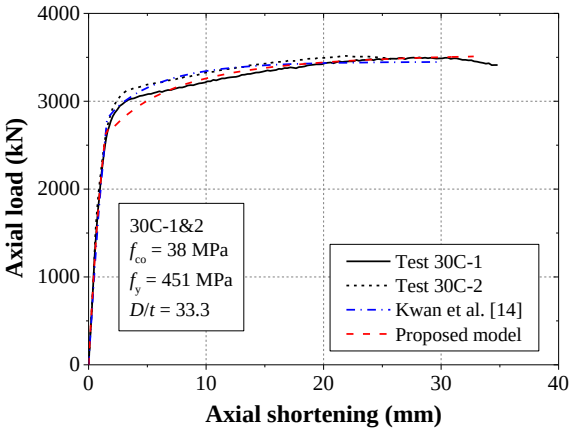

(e) Zhu and Chan [33], 30C

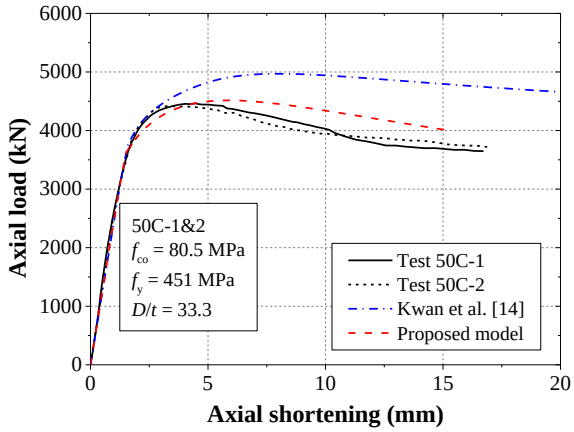

(f) Zhu and Chan [33], 50C

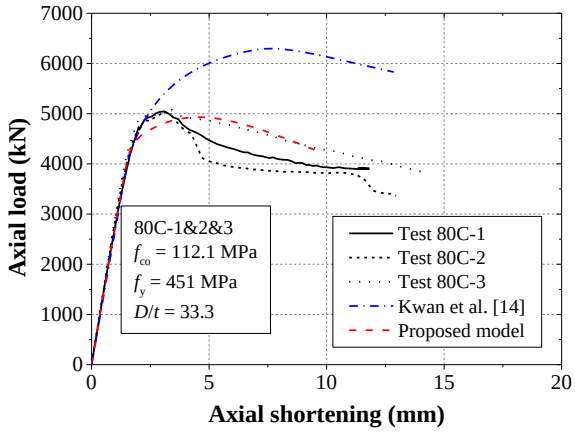

(g) Zhu and Chan [33], 80C

Figure 7. Assessment of load-axial shortening relationship of analytical model.

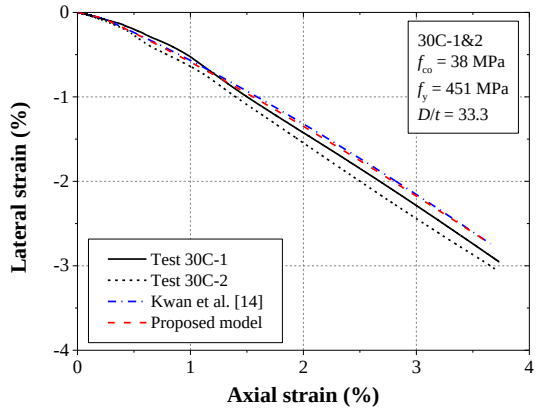

(a) Zhu and Chan [33], 30C

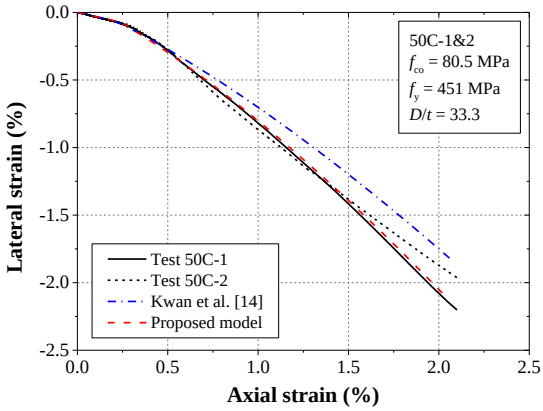

(b) Zhu and Chan [33], 50C

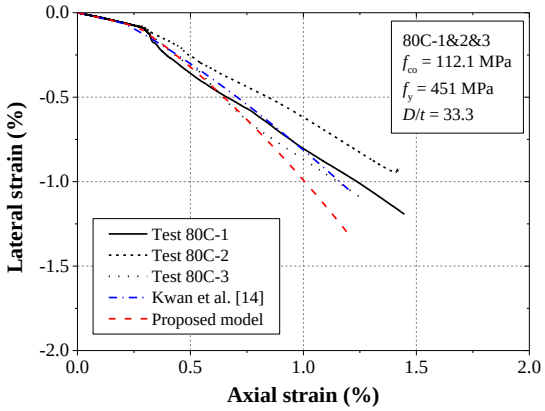

(c) Zhu and Chan [33], 80C

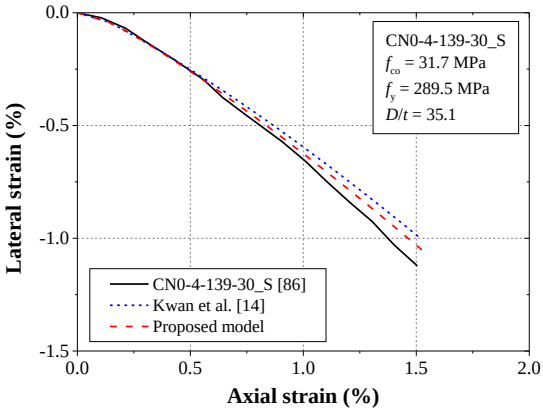

(d) Lai et al. [86], CN0-4-139-30_S

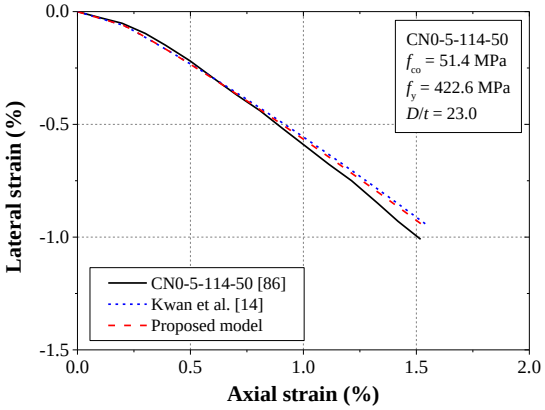

(e) Lai et al. [86], CN0-5-114-50

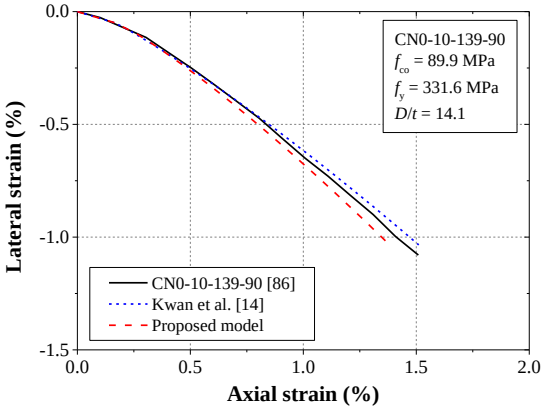

(f) Lai et al. [86], CN0-10-139-90

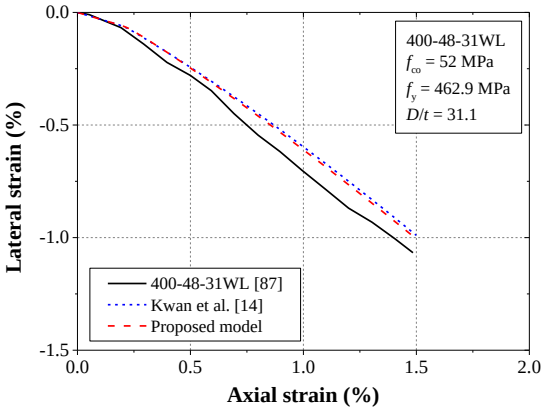

(g) Lin et al. [87], 400-48-31WL

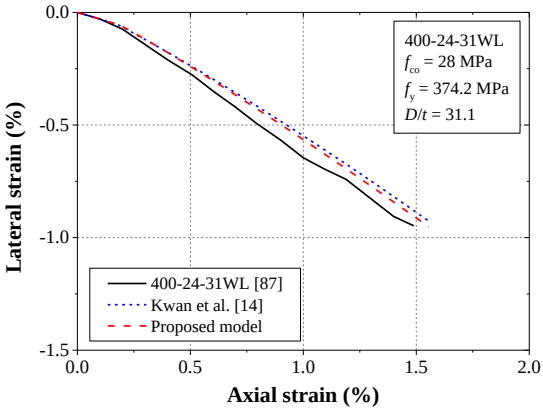

(h) Lin et al. [87], 400-24-31WL

Figure 8. Assessment of axial-lateral strain relationships of analytical model.

Table 1 Experimental data of Poisson's ratio at peak stress.

f_{co}	ε_{co}	$\varepsilon_{co,l}$	$\nu_{c,f}$
37.3	0.0023	0.0011	0.47
38.1	0.0022	0.0011	0.51
38.2	0.0027	0.0010	0.36
39.0	0.0022	0.0010	0.46
39.1	0.0022	0.0013	0.59
38.8	0.0022	0.0012	0.55
53.4	0.0023	0.0012	0.52
55.3	0.0023	0.0011	0.48
55.8	0.0024	0.0012	0.50
	Mean		**0.49**
	CoV		**0.06**
63.7	0.0028	0.0012	0.42
65.4	0.0030	0.0011	0.37
60.4	0.0025	0.0009	0.37
80.0	0.0027	0.0010	0.36
80.9	0.0026	0.0010	0.38
80.6	0.0026	0.0012	0.45
85.2	0.0030	0.0012	0.41
86.3	0.0031	0.0012	0.40
84.7	0.0029	0.0011	0.38
	Mean		**0.39**
	CoV		**0.07**
92.0	0.0025	0.00070	0.27
98.0	0.0027	0.00085	0.32
113.5	0.0030	0.00074	0.25
111.0	0.0030	0.00079	0.26
113.9	0.0031	0.00091	0.30
120.2	0.0032	0.00094	0.29
120.2	0.0031	0.00084	0.27
125.5	0.0034	0.00109	0.32
	Mean		**0.28**
	CoV		**0.09**

Table 2. Collected experimental data for the assessment of high strength circular concrete filled steel tubes

Specimens	f_{co} (MPa)	f_y (MPa)	D (mm)	t (mm)	$N_{u,test}$ (kN)	$N_{u,model}$ (kN)	ε_u	Confinement ratio
Han et al. [41]								
CA1-1	70	282	60	1.87	312	318	0.0090	0.55
CA1-2	70	282	60	1.87	320	318	0.0081	0.55
CA2-1	70	282	100	1.87	822	774	0.0060	0.32
CA2-2	70	282	100	1.87	845	774	0.0054	0.32
CA3-1	70	282	150	1.87	1701	1592	0.0053	0.21
CA3-2	70	282	150	1.87	1670	1592	0.0055	0.21
CA4-1	70	282	200	1.87	2783	2678	0.0048	0.16
CA4-2	70	282	200	1.87	2824	2678	0.0041	0.16
CA5-1	70	282	250	1.87	3950	4029	0.0038	0.12
CA5-2	70	282	250	1.87	4102	4029	0.0052	0.12
CB1-1	70	404	60	2	427	378	0.0086	0.85
CB1-2	70	404	60	2	415	378	0.0107	0.85
CB2-1	70	404	100	2	930	885	0.0050	0.49
CB2-2	70	404	100	2	920	885	0.0075	0.49
CB3-1	70	404	150	2	1870	1772	0.0050	0.32
CB3-2	70	404	150	2	1743	1772	0.0065	0.32
CB4-1	70	404	200	2	3020	2930	0.0046	0.24
CB4-2	70	404	200	2	3011	2930	0.0038	0.24
CB5-1	70	404	250	2	4442	4354	0.0041	0.19
CB5-2	70	404	250	2	4550	4354	0.0040	0.19
CC1-1	75	404	60	2	432	386	0.0085	0.80
CC1-2	75	404	60	2	437	386	0.0086	0.80
CC2-1	75	404	150	2	1980	1830	0.0047	0.30
CC2-2	75	404	150	2	1910	1830	0.0046	0.30
CC3-1	75	404	250	2	4720	4521	0.0036	0.18
CC3-2	75	404	250	2	4800	4521	0.0038	0.18
Zhu and Chan [33]								
50C-1	72.4	453	200	6	4463	4446	0.0085	0.73
50C-2	72.4	453	200	6	4423	4446	0.0073	0.73
80C-1	100.1	453	200	6	5071	5124	0.0064	0.53
80C-2	100.1	453	200	6	5040	5124	0.0059	0.53
80C-3	100.1	453	200	6	5099	5124	0.0058	0.53